NON-ROTATIONAL STATES IN ISOTONIC CHAINS OF HEAVY NUCLEI*

N.V. Antonenko, G.G. Adamian, L.A. Malov, A.N. Bezbakh
R.V. Jolos, V.G. Kartavenko

Joint Institute for Nuclear Research, 141980 Dubna, Russia

H. Lenske

Institut für Theoretische Physik der Justus-Liebig-Universität
35392 Giessen, Germany

(Received December 21, 2018)

The energies of low-lying non-rotational states are calculated taking into account the residual pairing and phonon–quasiparticle interactions. Two mean-field potentials, Woods–Saxon- and Skyrme-based potentials, are used. The hot fusion reactions ^{50}Ti+$^{247-249}$Bk and ^{51}V+$^{246-248}$Cm are compared for the synthesis of element 119.

DOI:10.5506/APhysPolBSupp.12.515

1. Introduction

Intensive experimental studies of superheavy nuclei [1–6] resulted in the discovery of new nuclei and obtaining the information on the single-particle states and nuclear deformations. The systematic calculations of single-particle spectra of heaviest nuclei have been performed in Refs. [7–10]. However, the interaction of quasiparticles with phonons, which is determined by the mean-field fluctuations, has not been taken into account there. To start this work, we used Refs. [9, 10] as a guide to the structure of heaviest nuclei. The numerous discussions with Adam Sobiczewski were also very valuable for getting the correct results.

Besides the self-consistent approach, the residual interaction is also considered in the Quasiparticle–Phonon Model (QPM) [11–13] which allows us to describe well the structure of deformed rare-earth nuclei and actinides. In this model, the nuclide chart is divided into a few regions around some

* Presented at the XXV Nuclear Physics Workshop "Structure and Dynamics of Atomic Nuclei", Kazimierz Dolny, Poland, September 25–30, 2018.

Z and A in which the parameters of the mean field and the residual interaction are fixed. To carry out the correct calculations for each nucleus, its equilibrium deformation has to be defined. This consistence is especially important when the calculations are performed for poorly studied nuclei. It is also important in the case of prediction of the properties of nuclei that are as yet uninvestigated.

2. Model

The QPM Hamiltonian [11] contains the central potential $V_{\rm WS}$ of the Woods–Saxon (WS) form for neutrons and protons, the spin–orbit part, the Coulomb field for protons, and the terms taking into account the interactions between quasiparticles. The parameters of the WS potential are given in Ref. [14]. Other parameters of the model are from Ref. [11].

The calculation of equilibrium deformations is carried out using the basis of the microscopic–macroscopic two-center shell model (TCSM) [16–18], taking into account the pairing and shell corrections. The single-particle states of the lower part of the TCSM spectrum for each deformation β_2 and β_4 are replaced by the corresponding states of the WS potential. With a good accuracy, the energy spectra in these potentials almost coincide [14].

The equilibrium deformation of the nucleus corresponds to the position of the minimum on the potential energy surface. In some cases, there exist additional local potential minima that can be interpreted as possible shape isomeric states of the nuclei. For example, in Fig. 1 for ^{286}Fl, there are two minima which differ in energy by approximately 0.9 MeV and have opposite signs of deformations.

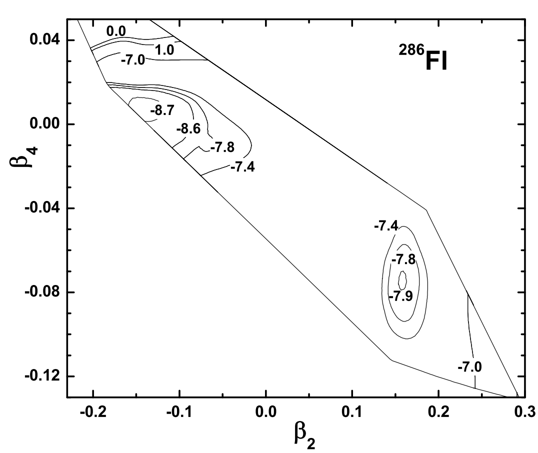

Fig. 1. Contour plot of the potential energy of ^{286}Fl as a function of β_2 and β_4. The energies are counted from the potential energy of spherical nucleus. There are two potential minima at $\beta_2 = -0.136$, $\beta_4 = 0.009$ and $\beta_2 = 0.161$, $\beta_4 = -0.074$.

3. Non-rotational states in isotonic chains

The single-particle spectra lying near the Fermi surface are used to calculate the non-rotational spectra and their quasiparticle–phonon structures with the QPM. The isotones with $N = 147$, 149, 151, 153, 155, 157, 159, and 161 are considered [14] to trace the dependence of low-lying non-rotational states on Z. In most cases, the model satisfactory describes the data, taking their uncertainties into account. A rather good agreement with the experimental data is seen in Figs. 2 and 3 presenting the calculated spectra for $N = 149$ and 151 isotones. The ground-state characteristics are correctly reproduced. As in Ref. [17], the energies of the level with the same Nilsson quantum numbers smoothly change with Z if the deformations of isotones are close to each other. In $N = 153$ isotones (Fig. 3), the spectra are quite dense near the ground states. Thus, the small change of the ground-state deformation could change the order of levels. Excepting a few cases, the experimental levels are well-described. Two first states $1/2^+$ and $7/2^+$ are close in energy. Therefore, the low-lying isomeric state is expected in $N = 153$ isotones.

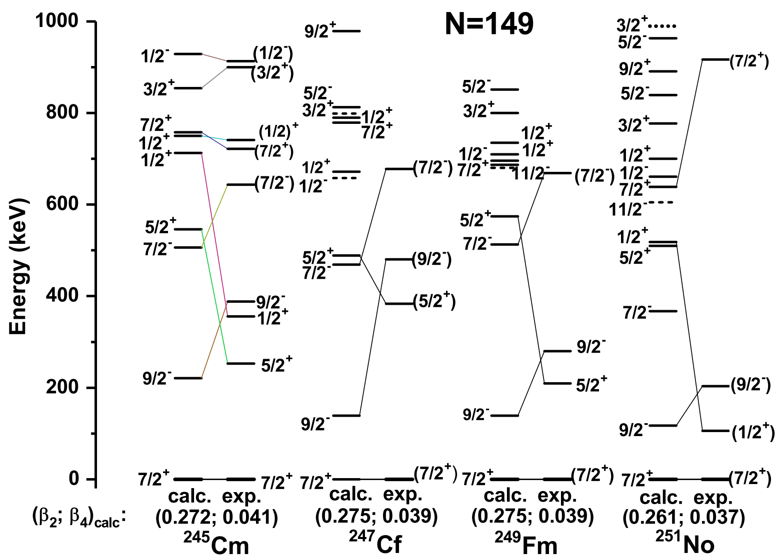

Fig. 2. Calculated spectra of low-lying states are compared with the available experimental data [15] for $N = 149$ isotones. The solid lines denote the states with one-quasiparticle component contributing more than 70% of the norm. The dotted lines correspond to the states with the quasiparticle⊗phonon component exceeding 70%. Other states are denoted by the dashed lines. The value of K in brackets means the tentative assignment.

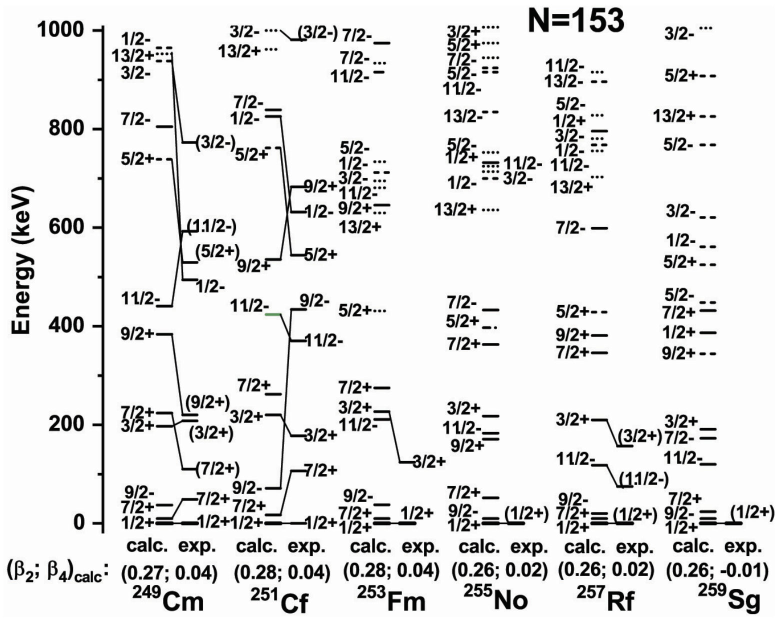

Fig. 3. The same as in Fig. 2, but for the $N = 153$ isotones.

The ground-state spin can change in the isotone chain if the deformation varies due to the cross of proton shell or sub-shell. The residual interaction and phonon coupling could also change the order of the quasiparticle levels in the case of the dense single-particle spectrum. For example, in the isotone chain with $N = 153$, the sequence of the close quasiparticle states $7/2^+[613]$ and $1/2^+[620]$ changes due to even small change of the ground-state deformation.

As shown, the effects beyond the mean-field influence the order of the levels in quite dense spectra. The phonon–quasiparticle interaction is important mainly for the states above 400 keV. Note that the calculations for all isotonic chains were performed with the fixed parameters of the Hamiltonian which seem to be reliable in the wide region of nuclear chart. If the lowest excited state differs by $\Delta K \geq 3$ with the ground state, one can expect an appearance of the isomeric state.

Let us compare the quasiparticle structures calculated with the self-consistent Skyrme–Hartree–Fock (SHF) approach and those calculated with the phenomenological Woods–Saxon single-particle potential at nuclear deformation found from the minimization of the sum of microscopic and macroscopic potential energies. Taking into account a possibility of the E1, E2, M1, and M2 γ-transitions between the excited states of the considered nuclei whose half-life times are shorter than the characteristic times T_α of the α-decays, and keeping only α-decays with shortest lifetimes, we have analyzed α-decay spectra and possible γ-transitions in nuclei of the α-decay chain of ^{285}Fl. The most probable α-decays are marked in Figs. 4 and 5 for the SHF-based and WS potentials together with the available experimental Q_α. The α-decays keeping the quantum numbers of the odd neutron are mainly taken into account. The probabilities of the allowed γ-transitions are estimated using the selection rules for the asymptotic quantum numbers.

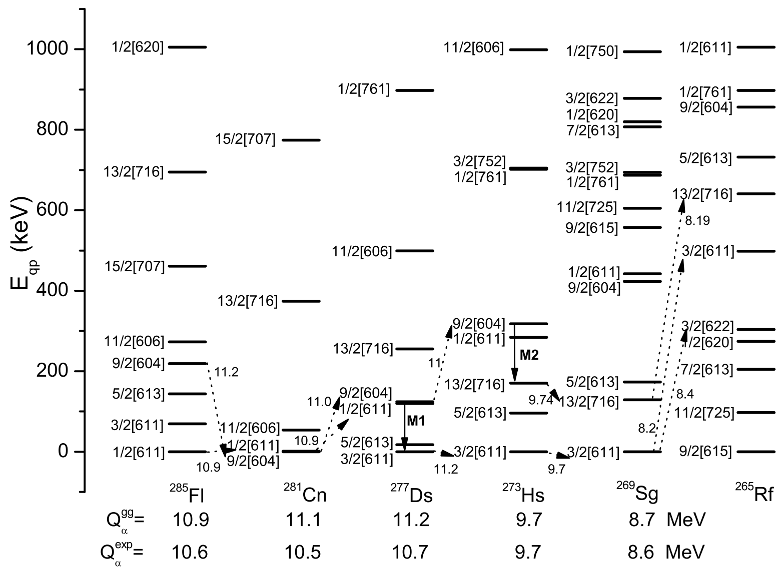

Fig. 4. The neutron one-quasiparticle spectra calculated within the SHF approach for the nuclei of the α-decay chain of ^{285}Fl. Q_α^{gg} is the α-decay energy for the ground-state-to-ground-state transition. $Q_\alpha^{\rm exp}$ is the experimental α-decay energy [19, 20].

The SHF-based calculations provide us with the nuclear binding energies and Q_α values for the ground-state-to-ground-state α-decays. In the case of the WS-based calculations, the Q_α values for the ground-state-to-ground-state α-decays are found as in Ref. [18].

As seen in Fig. 4, the state 9/2[604] could be the isomeric state in ^{285}Fl from which the α-decay can occur with $T_\alpha \approx 3$ ms because E2 transition to the state 5/2[613] is strongly suppressed. Within the WS approach, the state 15/2[707] goes down to become the isomeric state in Fig. 5. While in the SHF approach the isomeric state 1/2[611] is predicted in ^{281}Cn, in the WS approach the state 11/2[606] is expected to be the isomeric one (Fig. 5). The ground and isomeric states of ^{281}Cn are expected to be populated in the α-decay chain of ^{285}Fl. In Fig. 4, the α-decays of ^{281}Cn from the states 9/2[604] and 1/2[611] occur to the states with the same quantum numbers in

^{277}Ds. The M1 transition from the 1/2[611] state brings ^{277}Ds to the ground state. The E2 transition from the 9/2[604] state requires longer time than the indicated α-decay with $Q_\alpha \approx 11$ MeV and $T_\alpha \approx 0.5$ ms. Within the WS approach (Fig. 5), the α-decay of ^{281}Cn from the isomeric 11/2[606] state is forbidden because the 11/2[606] state in ^{277}Ds lays at quite high energy. Thus, the α-decay from this state likely populates either the ground or isomeric 3/2[611] state in ^{277}Ds after some γ-transitions. The α-decay of ^{277}Ds can occur from the isomeric and ground state (Figs. 4 and 5). In the SHF and WS approaches the ground 3/2[611] and isomeric 13/2[716] states of ^{273}Hs are populated in the α-decay chain of ^{285}Fl. The α-decays from these states populate the corresponding states in ^{269}Sg from which the α-decays with $T_\alpha > 410$ s occur and compete with the spontaneous fission. The α-decay of ^{265}Rf would need few hours, while the spontaneous fission requires about 1 min and interrupts the α-decay chain. The calculated values of Q_α seem to be close to the experimental data [19, 20].

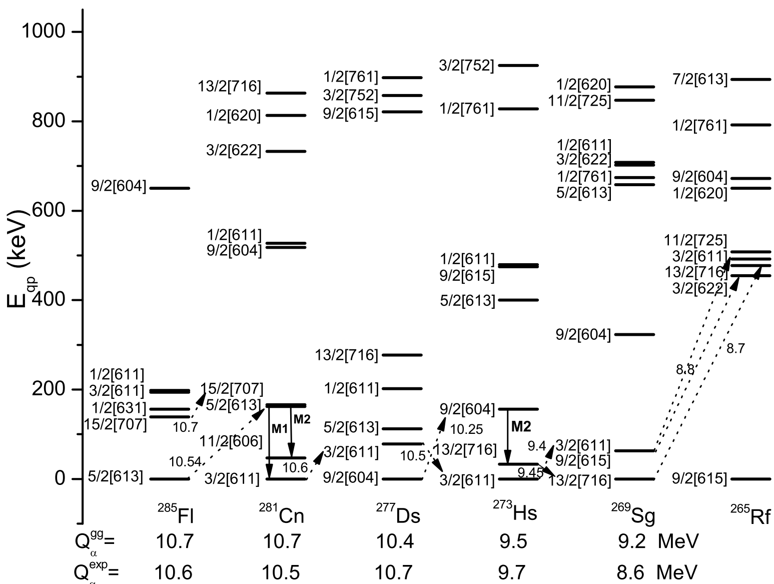

Fig. 5. The neutron one-quasiparticle spectra calculated within the WS approach for the nuclei of the α-decay chain of ^{285}Fl. $Q_\alpha^{\rm gg}$ is the α-decay energy for the ground-state-to-the ground-state transition. $Q_\alpha^{\rm exp}$ is the experimental α-decay energy [19, 20].

The calculations performed in the framework of the SHF and WS potentials demonstrate, as a rule, different orders of low-lying one-quasiparticle states [21]. However, the presence of isomeric states in heaviest nuclei as well as the values of Q_α are reliably predicted.

4. Estimates of production and structure of nuclei with $Z = 119$

In the dinuclear system (DNS) fusion model [22], the evaporation residue cross section in xn evaporation channel is determined as

$$\sigma_{\rm ER}^{xn}(E_{\rm cm}) = \sum_J \sigma_{\rm c}(E_{\rm cm}, J) P_{\rm CN}(E_{\rm cm}, J) W_{\rm sur}^{xn}(E_{\rm cm}, J)\,. \qquad (1)$$

The capture cross section $\sigma_{\rm c}(E_{\rm cm}, J)$ defines the transition of the colliding nuclei through the Coulomb barrier. The probability $P_{\rm CN}(E_{\rm cm}, J)$ of complete fusion and survival probability $W_{\rm sur}^{xn}(E_{\rm cm}, J)$ are calculated as in Ref. [23].

Using our predictions [18] of nuclear properties, we calculated the evaporation residue cross sections of the reactions ^{50}Ti+^{A}Bk (Fig. 6) and ^{51}V+ $^{A-1}$Cm (Fig. 7) leading to the compound nuclei with $Z = 119$ and the same mass number. As in Refs. [24–26], the isotopic dependence of $\sigma_{\rm ER}$ is rather weak in the treated interval of A. There is a certain interval of mass numbers of target nuclei where the product $P_{\rm CN}W_{\rm sur}$ changes weakly [24–26]. Indeed, the values of $\sigma_{\rm ER}$ are almost the same (about 40 fb) in the cases of ^{247}Bk and ^{249}Bk targets. In the reaction with ^{247}Bk, the loss in fission compensates the gain in fusion. In the case of ^{248}Bk target, the survival probability is smaller to those in the reactions ^{50}Ti+^{247,249}Bk. The decrease of $W_{\rm sur}^{xn}$ is partly negated by the increase of fusion and the maximum production cross section becomes about 22 fb. In the reactions ^{51}V+^{A}Cm, the value of $\sigma_{\rm ER}$ decreases by factor 2 with the mass number of target nucleus from $A = 248$ to $A = 246$. In the reactions ^{50}Ti+^{247}Bk→^{294}119+3n ($Q = -192.79$ MeV), ^{50}Ti+^{248}Bk→^{295}119+3n ($Q = -191.25$ MeV), and ^{50}Ti+^{249}Bk→^{295}119+4n ($Q = -190.13$ MeV), the nuclei ^{294,295}119 are predicted to be produced with the maximum cross sections. In the 4n evaporation channels of the reactions ^{51}V+^{246}Cm ($Q = -196.43$ MeV), ^{51}V+^{247}Cm ($Q = -194.57$ MeV), and ^{51}V+^{248}Cm ($Q = -193.36$ MeV), the predicted maximum production cross sections are about 6, 7, and 12 fb, respectively. The decrease of $\sigma_{\rm ER}$ with A is mostly because of the decrease of survival probability. As seen, $\sigma_{\rm ER}(^{50}{\rm Ti} +^{A} {\rm Bk})/\sigma_{\rm ER}(^{51}{\rm V} +^{A-1} {\rm Cm}) > 3$. Thus, for the production of nuclei with $Z = 119$, the reactions with the ^{50}Ti beam are favorable over those with ^{51}V.

In Fig. 8, the calculated one-quasiproton spectra and α-decays from the ground and possible isomeric states in the nuclei of the α-decay chain of the ^{295}119 element are shown. Almost all presented quasiparticle states of ^{295}119 are the hole states. The α-decay chain of the ^{295}119 contains ^{291}Ts and ^{287}Mc elements whose α-decay chains were treated in Ref. [27]. In Ref. [3], the α-decay of ^{271}Bh was observed in one chain. The calculated energies of α-decays of ^{287}Mc, ^{283}Nh, and ^{279}Rg are in a good agreement

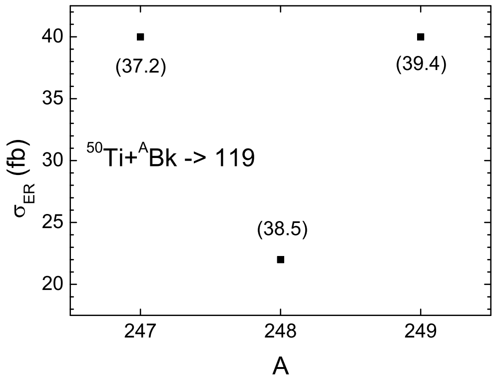

Fig. 6. Evaporation residue cross sections in the maxima of excitation functions of the reactions ^{50}Ti+^{A}Bk *versus* A. The excitation energies of compound nuclei in MeV are given in brackets. The ground-state mass excesses $M_{\rm th} = 206.85$, 207.9, and 208.85 MeV for the nuclei ^{297}119, ^{298}119, and ^{299}119, respectively, were used in the calculations.

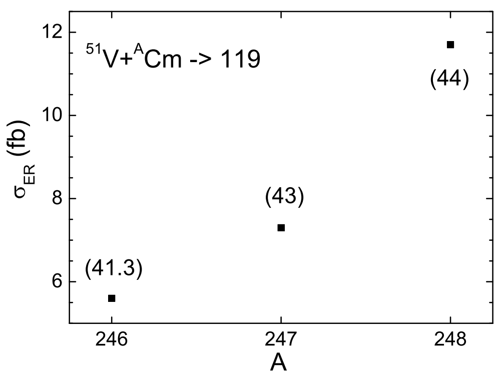

Fig. 7. The same as in Fig. 6, but for the reactions ^{51}V+^{A}Cm.

with the experimental data [3]. For the α-decay of ^{271}Bh, the calculated value of Q_α is underestimated by 0.47 MeV. Note that for this nucleus, we obtained $Q_\alpha = 9.02$ MeV close to $Q_\alpha = 9.07$ MeV in Ref. [28]. For ^{275}Mt, the K-allowed α-decays in Fig. 8 have Q_α values that are about 0.45 MeV smaller than $Q_\alpha^{\rm exp} = 10.48$ MeV [3]. However, the α-decay of ^{275}Mt to the states built on $9/2^+[624]$ state in ^{271}Bh has only $\Delta K = 1$ and cannot be excluded. In the case of this decay, $Q_\alpha \approx 10.28$ MeV and the agreement with the experiment becomes better. In ^{275}Mt, the estimated T_α is 4.2 ms with $Q_\alpha^{\rm exp} = 10.48$ MeV. However, $T_\alpha^{\rm exp} = 12^{+23}_{-5}$ ms that indicates some hindrance of this α-decay.

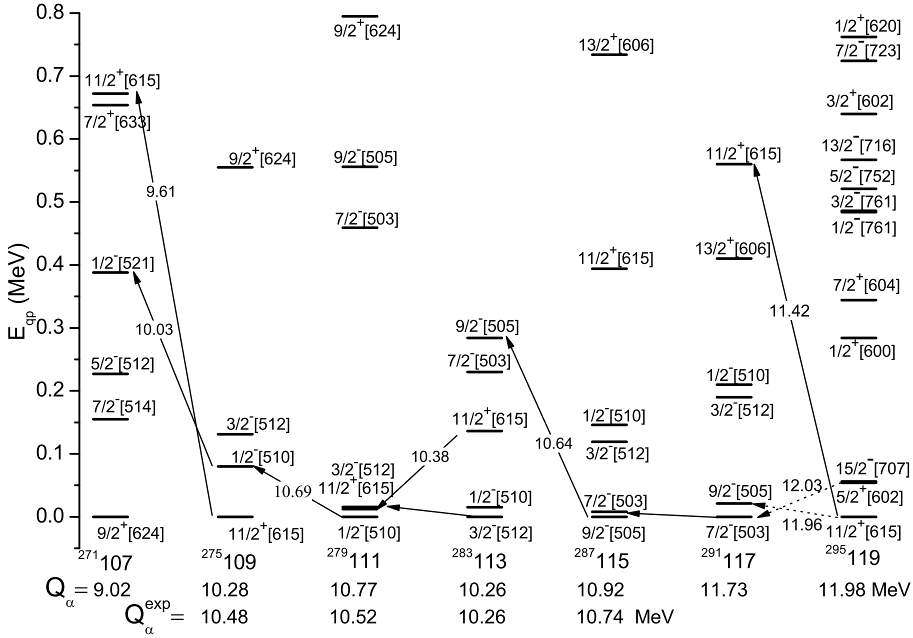

Fig. 8. Calculated energies $E_{\rm qp}$ of low-lying one-quasiproton states in the indicated nuclei of the α-decay chain of $^{295}119$. The calculated values of Q_α are for the ground-state-to-ground-state α-decay. Possible α-decays are traced by arrows. The experimental values of $Q_\alpha^{\rm exp}$ are from Ref. [1].

As seen in Fig. 8, in the evaporation residue $^{295}119$, the low-lying isomeric state $5/2^+[602]$ can be populated with a probability close to the population probability of the ground state. The same state in ^{291}Ts lies at quite high energy, $E_{\rm qp} > 0.8$ MeV. Therefore, the possible α-decay of $^{295}119$ from $5/2^+[602]$ state likely occurs into the ground state of ^{291}Ts with $\Delta K = 1$. This hindered α-decay is estimated to have half-life $T_\alpha > 20$ ms. The similar T_α is expected for the α-decay from the ground state of $^{295}119$ into the $9/2^-[505]$ state in ^{291}Ts. The K-allowed α-decay of $^{295}119$ from the ground state can occur with $Q_\alpha = 11.42$ MeV and $T_\alpha = 27$ ms.

In Ref. [27], we expected that the α-decay of ^{271}Bh occurs in about 9.3 s to ^{267}Db. The latest experiments [3] gave $T_\alpha = 1.2^{+5.9}_{-0.5}$ s. Thus, our predictions seem to be reasonable. The α-decay of ^{267}Db would need about 35 h that is too long in comparison with the time of spontaneous fission which occurs in about 1.8 h [3]. Therefore, the α-decay chain of $^{295}119$ or ^{291}Ts or ^{287}Mc is expected to be terminated by the spontaneous fission of ^{267}Db.

5. Summary

The systematic calculations of low-lying states were performed in the $N = 147$–161 isotones of heavy nuclei. The QPM was used to take into account the residual paring and phonon–quasiparticle interactions. This model was improved by finding out the ground-state deformations for each nucleus using the microscopic–macroscopic approach. As shown, the effects beyond the mean-field influence the order of the levels in quite dense spectra. The phonon–quasiparticle interaction is important mainly for the states above 400 keV. The calculations performed in the framework of the SHF and WS potentials demonstrate, as a rule, different orders of low-lying one-quasiparticle states. The α-decay occurs mainly between the one-quasiparticle states with the same quantum numbers in the mother and daughter nuclei. Therefore, some isomeric states are not populated in the α-decay chain. If our prediction of the structure of heaviest nuclei is correct, then one can expect the production of evaporation residues $Z = 119$ in the reactions ^{50}Ti+^{249}Bk and ^{51}V+^{248}Cm with the cross sections 40 and 12 fb, respectively.

This work was supported in part by RFBR (N 17-52-12015) and DFG. The Polish–JINR (Dubna) Cooperation Programmes are gratefully acknowledged.

REFERENCES

[1] Yu.Ts. Oganessian, *J. Phys. G* **34**, R165 (2007).
[2] Yu.Ts. Oganessian *et al.*, *Phys. Rev. Lett.* **104**, 142502 (2010).
[3] Yu.Ts. Oganessian *et al.*, *Phys. Rev. C* **87**, 014302 (2013).
[4] S. Hofmann *et al.*, *Eur. Phys. J. A* **32**, 251 (2007).
[5] F.P. Heßberger, *Eur. Phys. J. D* **45**, 33 (2007).
[6] B. Streicher *et al.*, *Eur. Phys. J. A* **45**, 275 (2010).
[7] S. Ćwiok, S. Hofmann, W. Nazarewicz, *Nucl. Phys. A* **573**, 356 (1994).
[8] S. Ćwiok, W. Nazarewicz, P.H. Heenen, *Phys. Rev. Lett.* **83**, 1108 (1999).
[9] A. Parkhomenko, A. Sobiczewski, *Acta Phys. Pol. B* **35**, 2447 (2004).
[10] A. Parkhomenko, A. Sobiczewski, *Acta Phys. Pol. B* **36**, 3115 (2005).
[11] V.G. Soloviev, *Theory of Complex Nuclei*, Oxford, Pergamon Press, 1976.
[12] N. Tsoneva *et al.*, *Phys. Rev. C* **61**, 044303 (2000).
[13] N. Van Giai, Ch. Stoyanov, V.V. Voronov, S. Fortier, *Phys. Rev. C* **53**, 730 (1996).

[14] G.G. Adamian, L.A. Malov, N.V. Antonenko, R.V. Jolos, *Phys. Rev. C* **97**, 034308 (2018).

[15] `http://www.nndc.bnl.gov/nndc/ensdf/`

[16] J. Maruhn, W. Greiner, *Z. Phys.* **251**, 431 (1972).

[17] G.G. Adamian *et al.*, *Phys. Rev. C* **84**, 024324 (2011).

[18] A.N. Kuzmina, G.G. Adamian, N.V. Antonenko, W. Scheid, *Phys. Rev. C* **85**, 014319 (2012).

[19] V.K. Utyonkov *et al.*, *Phys. Rev. C* **92**, 034609 (2015).

[20] P.A. Ellison *et al.*, *Phys. Rev. Lett.* **105**, 182701 (2010).

[21] V.G. Kartavenko *et al.*, *Chin. Phys. C* **41**, 074105 (2017).

[22] G.G. Adamian, N.V. Antonenko, W. Scheid, V.V. Volkov, *Nucl. Phys. A* **633**, 409 (1998).

[23] G.G. Adamian, N.V. Antonenko, H. Lenske, *Nucl. Phys. A* **970**, 22 (2018).

[24] G.G. Adamian, N.V. Antonenko, W. Scheid, *Phys. Rev. C* **69**, 011601(R) (2004).

[25] G.G. Adamian, N.V. Antonenko, W. Scheid, *Phys. Rev. C* **69**, 014607 (2004).

[26] G.G. Adamian, N.V. Antonenko, W. Scheid, *Phys. Rev. C* **69**, 044601 (2004).

[27] A.N. Kuzmina, G.G. Adamian, N.V. Antonenko, *Phys. Rev. C* **85**, 017302 (2012).

[28] I. Muntian, Z. Patyk, A. Sobiczewski, *Acta Phys. Pol. B* **32**, 691 (2001); **34**, 2141 (2003); I. Muntian, S. Hofmann, Z. Patyk, A. Sobiczewski, *Acta Phys. Pol. B* **34**, 2073 (2003); *Phys. At. Nucl.* **66**, 1015 (2003); A. Parkhomenko, I. Muntian, Z. Patyk, A. Sobiczewski, *Acta Phys. Pol. B* **34**, 2153 (2003); A. Parkhomenko, A. Sobiczewski, *Acta Phys. Pol. B* **36**, 3095 (2005).